International Journal of Nanoelectronics and Materials
Volume 11 (Special Issue) Dec 2018 [55-64]

Impact of Substrate Type on the Microstructure of H-Nb_2O_5 Thin Film at Room Temperature

Marwa K. Abood[1], Evan. T. Salim[1*] and Jehan A. Saimon[1]

[1]*Department of Applied Science, University of Technology, 10001 Baghdad, Iraq*

ABSTRACT

In this work the effect of substrate type on structural properties of the Nb2O5 thin films deposited on silicon and quartz substrate by spin coating technique is present. The formation of Nb2O5 thin films having an obvious polymorphous monocline structure. A significant enhanced was observed on the crystalline structure of films prepared on the silicon substrate, were more distinguished peaks comparing with quartz substrate was appeared. The structural the estimated structural constants reveal an increase in the estimated grain size of the prepared films on the silicon substrate. The lattice stress of the deposited films on Quartz and silicon was 0.19 and 0.15 respectively. Effect of number of deposited layers are also studied showing an increase in the absorbance, extinction coefficient (k), refractive index (n), optical conductivity, real (εr) and imaginary (εi) dielectric constant and decreasing in the band gap from (2.69) to (2.51) e.v as a result of increasing in the film number of layers from (3) to (6) layers.

Keywords: H-Nb_2O_5, Substrate Type, Structural, Optical, Morphological Properties.

1. INTRODUCTION

Superior performance of Nb_2O_5 had caused its intelligence applications such as energy band scheme and crystal phases' identification and alike. In specific, nanostructured Nb_2O_5 displays high surface to volume ratio and quantum confinement influences that allow individual physiochemical interactions at the films surface. As a results, morphological and nano doctrinaires meaningfully impact the optical and electronic characteristics of Nb_2O_5 films, leading to singular perceptions that are not observed in its bulk shapes.

Correspondingly, the Nb_2O_5 films characteristics enable as well be adjusted through other ways like the strange ions integration, crystal phase modulation and post composition heat treatment [1-10]. More newly, interest on Nb_2O_5 has acquired additional activity as a result of implementations other than catalysis and electrochromic. Particularly, thin films and nanostructured Nb_2O_5 have been used in solar cells, batteries and sensors [3, 11-13].

Because of its large band gap, Nb2O5 is a transparent, air-stabilized and water-indissoluble solid material with a comparatively complex structure that exhibits spacious polymorphic. There are nearly 15 polymorphism shapes of Nb_2O_5 that have yet been apprised, while, the generality popular crystal phases are mostly pseudo-hexagonal, orthorhombic, and monoclinic (H-Nb_2O_5) structures [9, 14-16].

Relying on the crystallinity of Nb2O5 films they can effectively absorb light in the UV wavelength regions. Tunability of Nb_2O_5 band gap is conceivable and factors like stoichiometry, heat treatment, crystallinity and integrated strange ions can impact dramatically the energy band gap [17-20].

* Corresponding Author: *evan_tarq@yahoo.com.*

In this work, effect of substrate type on the structural properties of Nb_2O_5 thin films, and optical properties of films prepared on quartz substrate with different layers Number was investigated.

2. MATERIAL AND METHODS

Niobium pentoxide chemical solution was obtained by using 0.2 g M-Nb_2O_5 micro powder 99.99% ultrahigh-purity, mixing with ((DIW, ethanol, HF, NH_3OH) having (1:1:4:8) molar ratio. In water bath 100 ^oC the HF was added to Nb_2O_5 and stirring for 1 hour until the powder entirely disappears leaving a transparent solution. This was followed by the required ammonia NH3OH which insure the formation of Nb2O5 colloidal solution according to Eq. (2). Finally a milky like colloidal solution was obtained. All above chemical reactions take the following chemical formulas [21, 22]

$$Nb_2O_5 + 10HF \rightarrow 2H_2\left[NbOF_5\right] + 3H_2O \quad (1)$$

$$2H_2[NbOF_5] + 10NH_4OH \rightarrow Nb_2O_5 \downarrow + 10NH4F + 7H_2O \quad (2)$$

A spin coating method was used to prepare the Nb_2O_5 thin films. A spinning speed of about 2500 rpm was depended to deposit the chemical solution on both substrates. An 80^oC was depended as heating temperature for one min to dry the prepared films. No farther heat treatment was used.

Two different number of deposited layers (N1=3, N2=6) resulting in two different films thicknesses on the quartz substrate, and (N1=3) for silicon substrate, were similar effect for the deposited layer number were observed on both substrate. The structural properties were studied using x-ray diffraction instrument from (Shimadzu 6000).

The optical properties were measured using Uv-visible spectrophotometer from (T60 UV-Vis). Morphological properties of prepared sample at higher thickness were achieved employing SEM of (AA-3000) type.

In this work, substrate type effect on structural properties of the mono-clink (H- Nb_2O_5) thin film prepared using colloidal solution at room temperature was studied. Also, the effect of the deposited layer number on the optical and morphological properties of films prepared on Quartz substrate was investigated.

3. RESULT AND DISCUSSION

3.1 Structural Studies

Figure (1) presents the XRD diffraction peaks of the sample before adding ammonia showing its crystal structure and orientation.

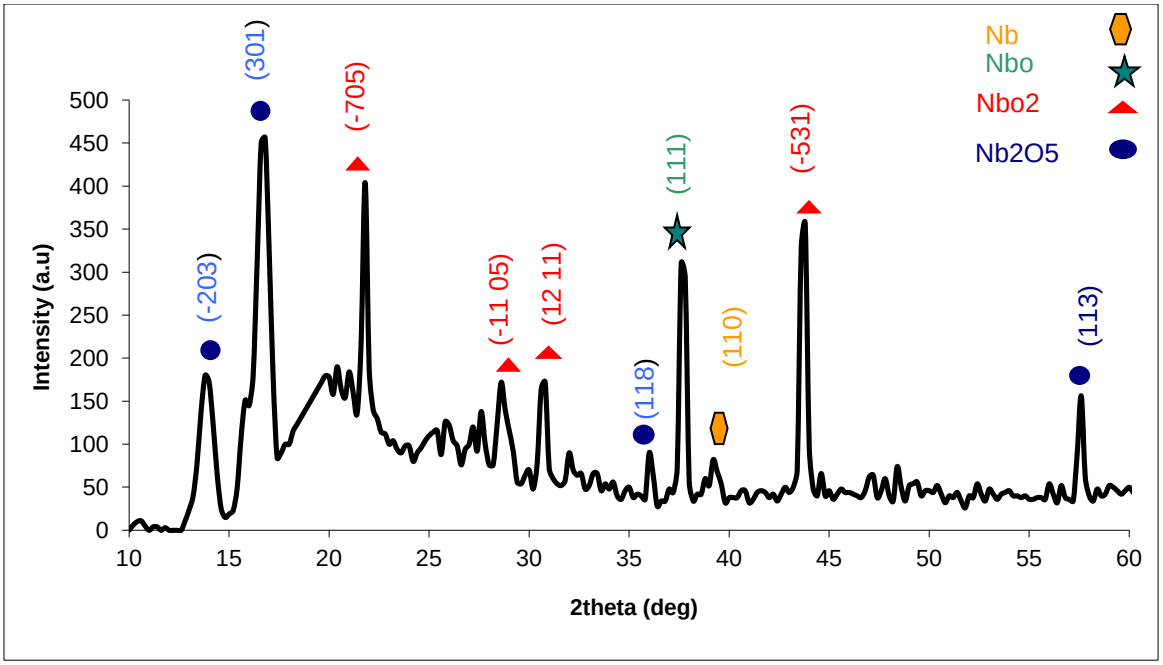

Figure 1. XRD results of prepared film before adding ammonia.

These results ensure the complete desolation of the raw material. The obtained diffraction peaks were related to different niobium oxide phases. It's also presence the existence of niobium metal as well as higher order niobium oxidation in different phases (Nb, NbO, NbO_2, Nb_2O_5, Nb_3O_7). However, NbO phase was the dominated one.

The diffraction peaks found to be at (21.80, 28.60, 30.80, 37.80, 43.80, 57.60) which directly related to the (-705), (-11 05), (12 11), (111), (-531) and (113) diffraction plains respectively.

A dramatic change in the structure was achieved when the ammonia was added as shown in figure (2). In the last figure, the obtained results prove the formation of polymorphous Nb_2O_5 structure. A clear enhanced in the crystalline structure was achieved with distinct peaks for the film deposited on the silicon substrate in comparison with quartz substrate. The dominated diffraction peaks on both substrates were corresponding to (301) and (111) diffraction plain; this means that the formatted structure was monoclinic crystalline (H- phase) at both substrates.

A diffraction plane belongs to (NbO) diffraction peak was observed for films prepared on both substrates. Diffraction peaks at (101) and (011) diffraction planes were recognized for films prepared on both substrates respectively, with lower intensity at quartz substrate.

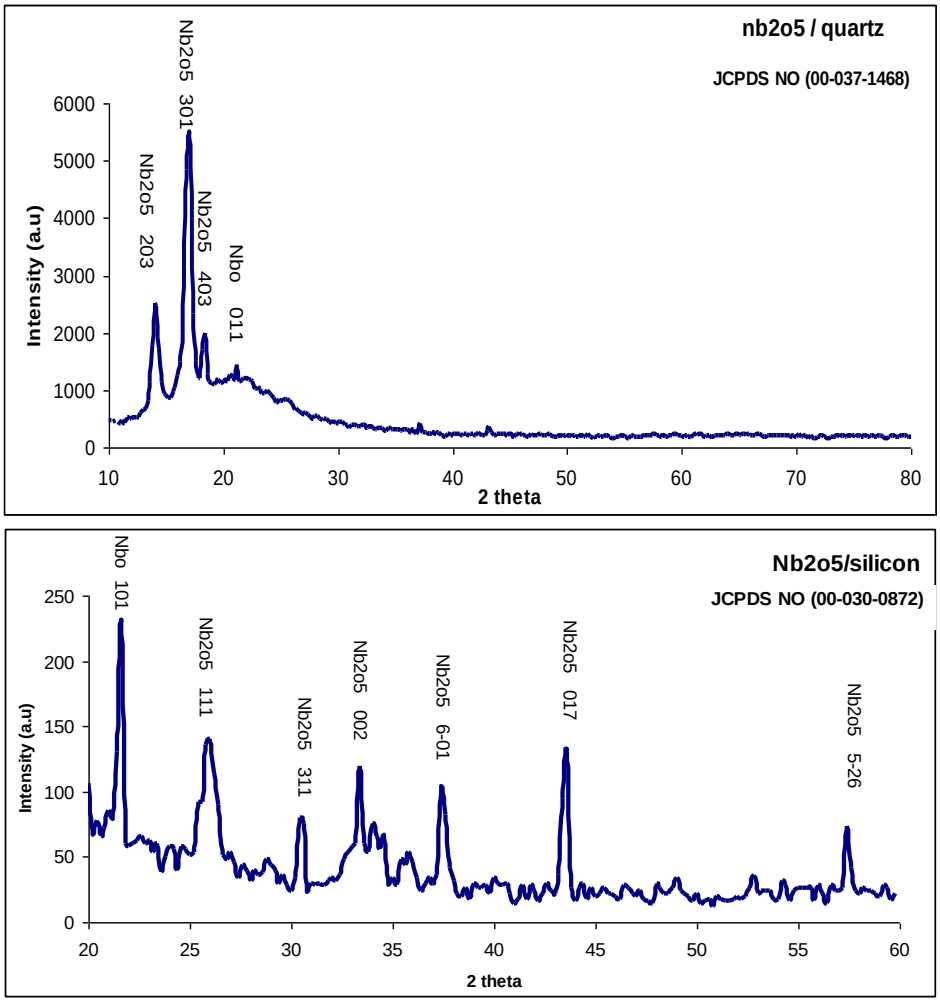

Figure 2. XRD results of the prepared films (a) quartz substrate (b) Si substrate.

The constant parameters that distinguish the structural properties of the deposited films were characterized by analyzing of XRD results using the following equations, were listed in the table (1):

$$D = \frac{K\lambda}{\beta \cos\theta}. \quad (3)$$

$$\delta = \frac{1}{D^2} \quad (4)$$

$$\varepsilon = \frac{\beta}{4\tan\theta} \quad (5)$$

Where D (nm) represents the grain size, K is constant depended on the wave length used, β is the full FWHM of the peak, Θ is the Bragg angle, δ is the density of dislocation, and ε is the stress [23-25].

The parameters extracted from X- Ray diffraction analysis listed in table 1 shows that the film deposited on quartz substrate has a smaller grain size compared to deposited films on silicon,

while the dislocation density found to have a larger, which give an indication that films prepared on silicon have higher quality and show an improved structure. In addition, the average value of stress found to have lower value for film deposited on quartz substrate (0.15) compared with the films deposited on silicon substrate which found to be about (0.19). These results may be related to the presence of a preferred orientation at the Si substrate similar results could be found else were [26].

3.2 Optical Studies

By using the UV-visible spectrophotometer, the optical absorption of the prepared films on the quartz substrate as a function of wavelength was characterized. From figure (3) it is obvious that the absorbance intensity directly related to the number of a deposited layer. This behavior may attribute to the increase of Nb_2O_5 micro particles per unit volume of the films; this has the good agreement with other work [27]. By using Tauc equation [28], the energy gap of the deposited film can be measured depending on the absorption spectrum.

$$\alpha_{h\nu} = A(h\nu - E_g)^2 \tag{6}$$

where α is the absorption coefficient, A is a constant, h is the Planck's constant, μ is the photon frequency, Eg is the optical energy gap and r is a constant, its value chosen depending on the transition type, due to the direct allowed transition in [29] Nb_2O_5 the power value is (1/2).

Table 1 The estimated structural constants of the prepared films

	Peaks (deg)	**d-spacing (A)**	**hkl**	**B (deg)**	**D (nm)**	**(δ) *10-3 (line/m2)**	**ε**
Silicon	21.2	4.11	011	0.44	19.2	2.71	0.28
	26.0	3.42	111	0.40	21.3	2.20	0.21
	30.6	2.9	311	0.44	19.5	2.61	0.13
	33.4	2.6	002	0.70	12.3	6.52	0.21
	37.4	2.39	601	0.52	16.7	3.55	0.17
	43.6	2.07	017	0.50	17.8	3.13	0.13
	57.4	1.6	526	0.45	21.0	2.26	0.21
average					18.3	3.28	0.19
Quartz	14.0		203	0.60	13.9	5.14	0.15
	17.0	5.2	301	0.70	11.9	6.95	0.18
	18.4	4.8	403	0.40	21.0	2.26	0.11
average					15.6	4.79	0.15

Figure (4) shows that the energy gap value decreased with increasing of the number of layer from (2.69) to (2.51) e.v when the number of layers increased from 3 to 6 layers, this reduction due to the enhancement in the crystals, changing in the surface morphology of the deposited film and changing in the atomic distances finally due to defects existing in the films [27].

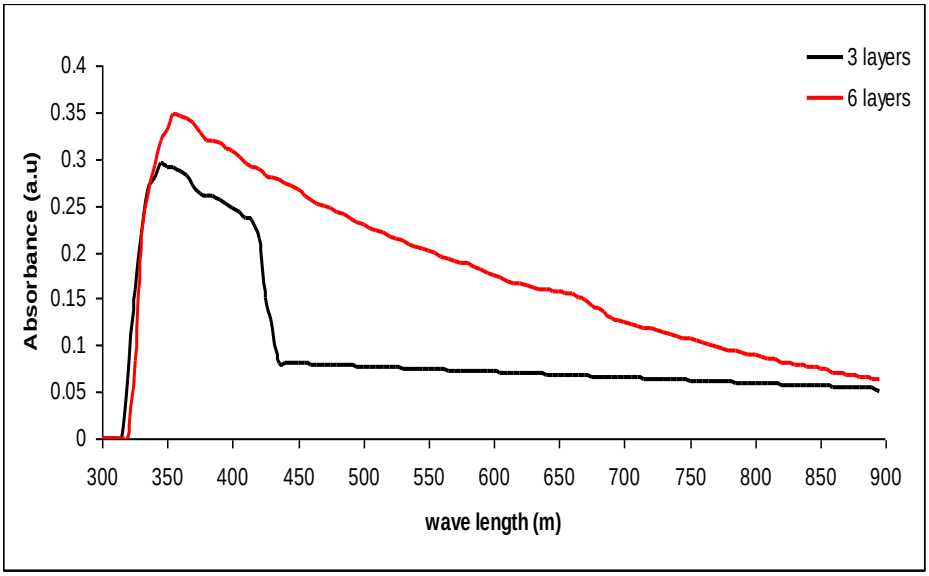

Figure 3. The absorbance Vs. wavelength at two different layers number.

The relation between (αhν)2 versus (hν) (Tauc plot), the extrapolation of the linear parts with photon energy would give the value of Eg as shown in figure (4).

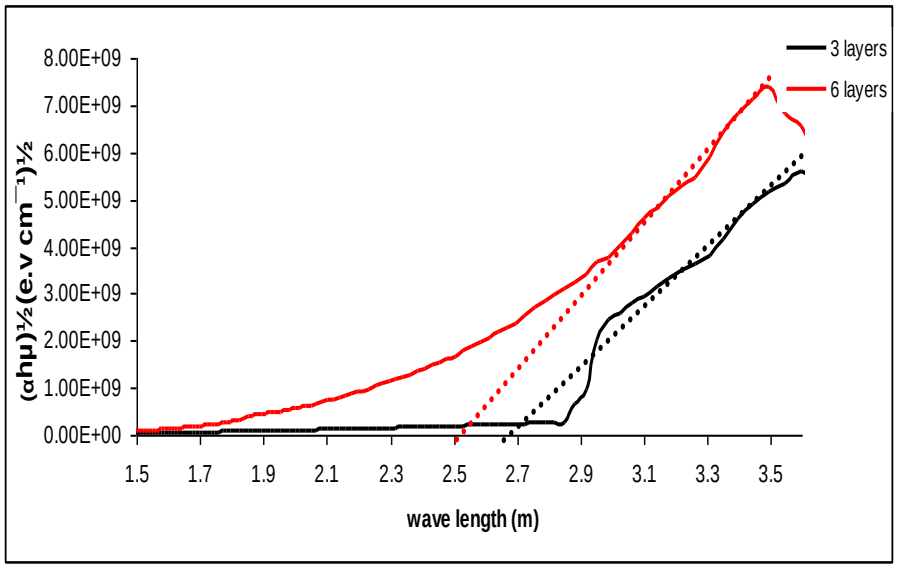

Figure 4. Energy gap of Nb_2O_5 films with two different deposited layer number.

Extinction coefficient (k), refractive index (n), optical conductivity, real (εr) imaginary (εi) dielectric constant are also measured depending on the optical properties resulted from analysis using the following formulas and represented in figure (5).

$$K = \frac{\alpha\lambda}{4\pi} \tag{7}$$

$$n = \frac{1+R}{1-R}\sqrt{\frac{4R}{(1-R)^2} - K^2} \tag{8}$$

$$\sigma = \frac{\alpha n}{4} \tag{9}$$

$$\varepsilon_r = n^2 - K^2 \tag{10}$$

$$\varepsilon_i = 2nK \tag{11}$$

where λ is the wave length of the incident photon [30-33].

The relation between the photon wave length and the extinction coefficient and the refractive index is shown in figure 5(A&B). It is obvious there value decreased with wave length increasing and increased with the increasing of the number of layers. There decreasing may attribute to the increase of the absorption showing a normal dispersion of the film. While the increase of extinction coefficient is due to the changing of the polarization of the thin films, also, the increase in the refractive index as the number of the layers increasing is due to particles compactness and aggregation [34-35].

The variation of optical conductivity with the photon wave length is shown in figure 5 (C). From this figure, it is clear that the optical conductivity increased with the increase of the wave length for a different number of layers. This increasing may attribute to the increase in the density of state in the band gap.

The relation of both εr and εi with λ for thin films under consideration is shown in Figure 5 (D&E) for thin films at different layer number. It was clear that real and imaginary parts of the dielectric constant were increases with the increase of the photon wave length and this is associated with how much the velocity of the photon retard inside the material and gives the indication about the losing of energy of a charged particle which passed through the material [37].

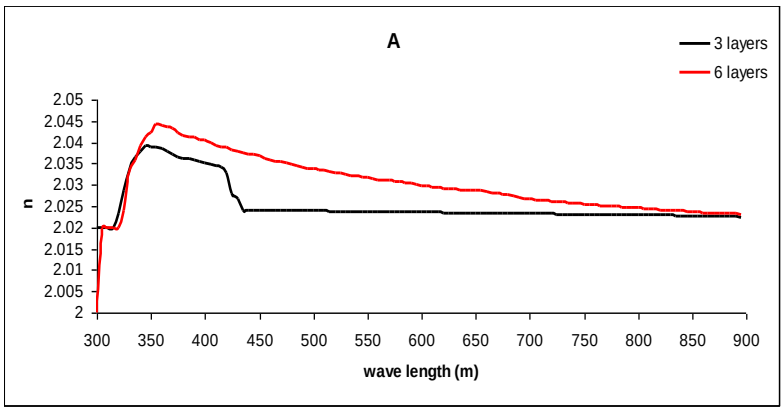

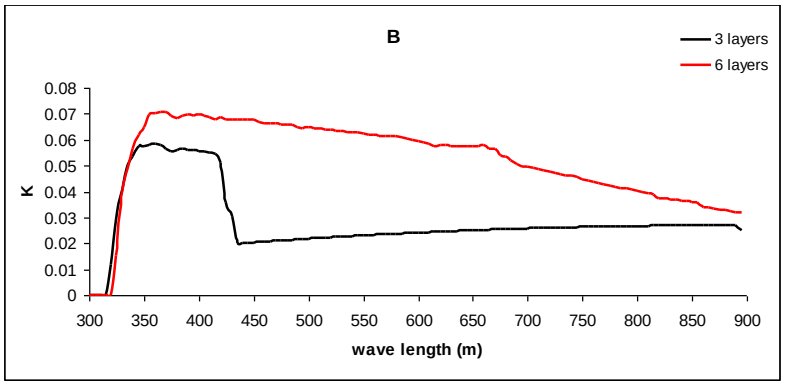

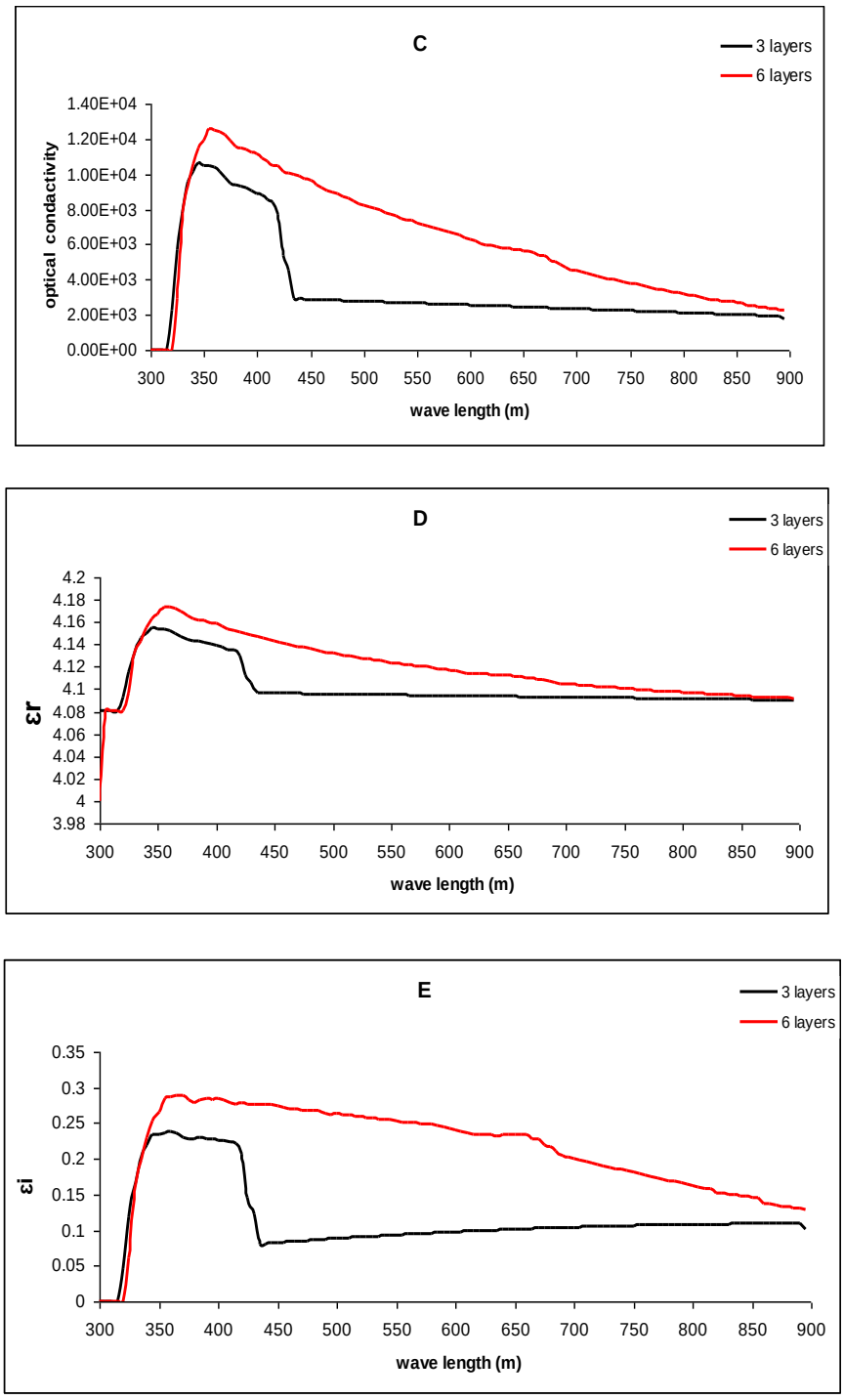

Figure 5. Relation between the photon wave length and refractive index (A), extinction coefficient (B), optical conductivity (C), real (D) and imaginary (E) dielectric coefficient.

3.3 Morphological Studies

The morphological properties of the Nb_2O_5 films prepared on the quartz substrate is shown in figure 6 (a & b). The formation of homogeneous microstructure thin film could be recognize with presents of rock like structures along the surface of the film, the obtained structure is a normal formatted on films deposited by chemical method [38-40].

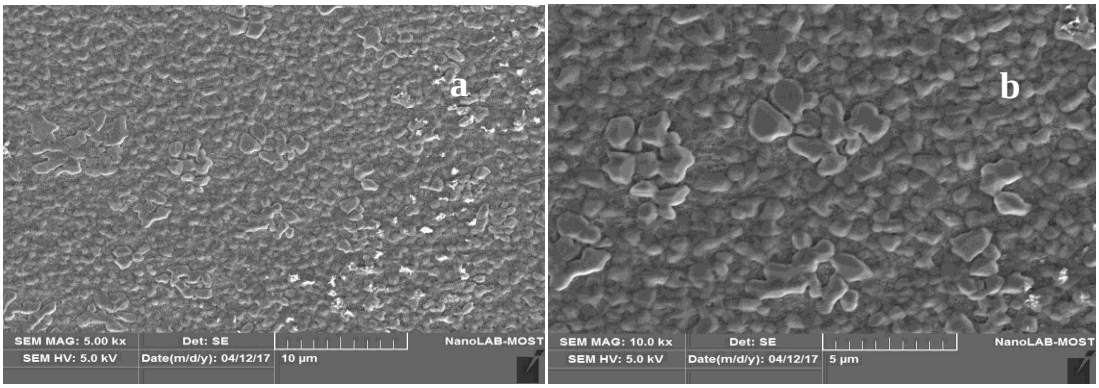

Figure 6. SEM micrograph of films film prepared on quartz substrate.

4. CONCLUSION

As a raw niobic acid based colloidal solution was successfully used to prepare Nb_2O_5 thin films at room temperature with no further heat treatment. This was ensured by the X- Ray diffraction peaks which related to H (mono-clink) structure. The structural parameters show that quartz substrate gives Nb_2O_5 film with smaller grain size and lower stress, but higher dislocation density. The number of deposited layers effect is likewise studied showing growth in the absorbance and reduction in the band gap as a result of the increase in the deposited layers.

REFERENCE

[1] M. Li, X. He, Y. Zeang, M. Chen, Z. Zhang, H. Yang, P. Fang, X. Lu & Y. Tong, Chem. Sci. **6**, 12 (2015) 6799-6805.
[2] Makram A. Fakhri, Evan T. Salim, M. H. A. Wahid, U. Hashim, Zaid T. Salim, Journal of Materials Science: Materials in Electronics. **29**, 11 (2018) 9200-9208.
[3] G. C. Vezzoli, Phys. Rev. B. **26** (1982) 3954-3957.
[4] R. Ghosh, M. K. Brennaman, T. Uher, M. Ok, E. T. Samulski, L. E. McNeil, T. J. Meyer & R. Lopez, ACS Appl. Mater. Interfaces. **3**, 10 (2011) 3929–3935.
[5] A. Le Viet, R. Jose, M. V. Reddy, B. V. R. Chowdari & S. Ramakrishna, J. Phys. Chem. C **114**, 49 (2010) 21795–21800.
[6] J. Z. Ou, R. A. Rani, M. H. Ham, M. R. Field, Y. Zhang, H. Zheng, P. Reece, S. Zhuiykov, S. Sriram, M. Bhaskaran, R. B. Kaner & K. Kalantar-zadeh, ACS Nano **6**, 5 (2012) 4045–4053.
[7] X. Fang, L. Hu, K. Huo, B. Gao, L. Zhao, M. Liao, P. K. Chu, Y. Bando, D. Golberg, Adv. Funct. Mater. **21**, 20 (2011) 3907–3915.
[8] S. Qi, R. Zuo, Y. Liu, Y. Wang, Mater. Res. Bull. **48** (2013) 1213–1217.
[9] C. Nico, T. Monteiro, M. P. F. Gracca, Prog. Mater. Sci. **80** (2016) 1–37.
[10] A. G. S. Prado, L. B. Bolzon, C. P. Pedroso, A. O. Moura, L. L. Costa, Appl. Catal. B **82** (2008) 219-224.
[11] A. M. Ferrari-Lima, R. G. Marques, M. L. Gimenes, N. R. C. Fernandes-Machado, Catal. Today. **254** (2015) 119-128.
[12] H. A. J. L. Mourão, V. R. Mendonça, A. R. Malagutti, C. Ribeiro, Quim. Nova **32**, 8 (2009) 2181-2190.
[13] I. Sieber, H. Hilderbrand, A. Friedrich, P. Schmuki, Electrochem. Commun. **7**, 1 (2005) 97-100.
[14] P. Viswanathamurthi, N. Bhattarai, H. Y. Kim, D. R. Lee, S. R. Kim, M. A. Morris, Chem. Phys. Lett. **374**, 1 (2003) 79-84.
[15] J. Son, J. Wang, F. E. Osterloh, P. Yu & W. H. Casey, Chem. Commun. **50** (2014) 836-838.

[16] M. Schmitt, S. Heusing, M. A. Aegerter, A. Pawlicka, C. Avellaneda, Sol. Energy Mater. Sol. Cells, **54**, 1 (1998) 9-17.
[17] Z. Weibin, W. Weidong, W. Xueming, C. Xinlu, Y. Dawei, S. Changle, P. Liping, W. Yuying & B. Li, Surf. Interface Anal. **45**, 8 (2013) 1206–1210.
[18] O. D. Coskun & S. Demirela, Appl. Surf. Sci. **277** (2013) 35– 39.
[19] S. Lee, J. Kwon, J. Ahn, J. Park,. Ceramics International **43**, (2017) 6580–6584.
[20] M. R. Joya, J. J. B. Ortega, A. M. R. Paez, J. G. da S. Filho & P. de T. C. Freire, Metals **7** (2017) 142.
[21] O. S. Ayanda & F A Adekola, Journal of Minerals & Materials Characterization & Engineering **10**, 3 (2011) 245-256.
[22] N. Izabela & Z Maria, Chemical Reviews**. 99**, 12 (1999) 3603–3624.
[23] A. Singh & H. Vishwakarma, Materials Science-Poland **33**, 4 (2015) 751-759.
[24] F.M. Tezel & İ. A. Kariper, Materials Science-Poland **35**, 1 (2017) 87-93.
[25] Z. T. Salim, U. Hashim, M. K. M. Arshad, M. A. Fakhri, Int. J. Appl. Eng. Res. **11** (2016) 8785–8790.
[26] M. K. Abood, E. T. Salim J. A. Saimon, International Journal of Nanoelectronics and Materials. **11**, 2 (2018) 127-134.
[27] Y. Akaltun, M. A. Yıldırım, A. Ateş & M. Yıldırım, Optics Communications **284**, 9 (2011) 2307-2311.
[28] Evan T. Salem, Ibrahim R. Agool & Marwa A. Hassan, International Journal of Modern Physics B. **25**, 29 (2011) 3863–3869.
[29] Y. Wang, S. Dai, F. Chen, T. Xu & Q. Nie, Materials Chemistry and Physics **113**, 1 (2009) 407-411.
[30] M. A. Muhsien, E. T. Salem, I. R. Agool, H. H. Hamdan, Appl. Nanosci. **4**, 6 (2014) 719–732.
[31] E. T. Salim, S. M. Al Wazny, M. A. Fakhri, Mod. Phys. Lett. B **27** (2013) 1350122-7–1350122-1.
[32] Makram A Fakhri, Evan T Salim, Ahmed W Abdul Wahhab, U Hashim, Zaid T Salim, Optics Laser Technology. **103** (2018) 226-232
[33] E. T. Salim, M. A. Fakhri, H. Hasan, Int. J. Nanoelectron. Mater. **6** (2013) 121–128.
[34] M. A. Fakhri, Y. Al-Douri, U. Hashim, E. T. Salim, Adv. Mater. Res. **1133** (2016) 457–461.
[35] Z. T. Salim, U. Hashim, M. K. M. Arshad, M. A. Fakhri, E. T. Salim,. Mater. Res. Bull. **86** (2017) 215–219.
[36] M. A. Fakhri, U. Hashim, E. T. Salim, Z. T. Salim, J. Mater. Sci. Mat. In Elec. **27**, 12 (2016) 13105–13112.
[37] D. Singh, S. Kumar, R. Thangaraj & T. Sathiaraj, Physica B: Condensed Matter. **408** (2013) 119-125.
[38] A. Verma & P. K. Singh, Indian Journal of chemistry. **52A** (2013) 593-598.
[39] M. K. Abood, M. H. A. Wahid, E. T. Salim J. A. Saimon, EPJ Web of Conferences **162** (2017) 01058.
[40] Evan T. Salim, Jehan A. Saimon, M. K Abood, M. A. Fakhri, Mater. Res. Express **4** (2017) 106407.